The alternative irregularity reduction algorithm built on 2-stage identification with AMF on FMIO

Vorapoj Patanavijit[1], Darun Kesrarat[2], Kornkamol Thakulsukanant[3]
[1]Faculty School of Engineering, Assumption University of Thailand, Bangkok, Thailand
[2]Faculty School of Science and Technology, Assumption University of Thailand, Bangkok, Thailand
[3]Martin de Tours School of Management and Economics, Assumption University of Thailand, Bangkok, Thailand

Article Info

Article history:

Received Mar 15, 2022
Revised Sep 12, 2022
Accepted Sep 19, 2022

Keywords:

2-stage identification
Adaptive median filter
Digital image denoising
Digital image processing
FMIO
RMIO
Standard median filter

ABSTRACT

Built on neighborhood correlation, a 2-stage identification technique was offered to incorporate on the irregularity reduction algorithm for random magnitude impulse outlier (RMIO). As a result, this algorithm has an ultimate efficacy thereby a 2-stage identification technique becomes to be one of the high efficacy identification technique. Accordingly, this paper attempts to propose an alternative irregularity reduction algorithm built on a 2-stage identification and adaptive median filter (AMF) with under fix magnitude impulsive outlier (FMIO) at little, mild and immense massiveness. First, by examining great number of depictions, the optimized window dimension for 2-stage scheme from computation and performance is disposed. Second, comprehensive examinations represent that the 2-stage identification technique is disposed to identify between regular and irregular pixels at all massiveness, especially little and mild massiveness. Third, the identification efficacy on great depictions at all massiveness is examined on regular, irregular, regular-irregular efficacy perspective to estimate the optimal window size and optimal 2-stage constant value. Finally, the overall outlier reduction efficacy of an outlier reduction built on 2-stage technique and AMF is examined on great depictions at all massiveness related with other up-to-the-minute outlier reductions. From these results, the outlier reduction has remarkable efficacy than other up-to-the-minute outlier reductions.

Corresponding Author:

Vorapoj Patanavijit
Faculty School of Engineering, Assumption University of Thailand
88 Moo 8 Bang Na-Trad Km. 26, Bang Sao Thong, Samut Prakan 10570, Thailand
Email: patanavijit@yahoo.com

1. INTRODUCTION

In present's contemporary era of multimedia and digital image processing [1], there are enormous contemporary utilizations on digital depictions [2]-[5] in last fifteen years therefrom one of the fundamental procedures for multimedia utilizations [5] for instant face arrangement [6], SR enhancement from various depictions [7], [8], and SR enhancement from one depiction [9], is the irregularity reduction algorithm for the ground that contemporary multimedia utilizations [5]-[9] are commonly conscious on irregularity. By ordinary, the irregularity reduction algorithm [10]-[21] is the fundamental procedures, which must be initially executed before contemporary multimedia utilizations [5]-[9] for the ground that the capableness of contemporary multimedia utilizations is regularly impaired when the applied digital depictions are highly incorporated of irregularity data (so called outlier). In due cause, the irregularity reduction algorithm is a necessarily fundamental procedure for MRI depiction, submerged water depiction, and biometric depiction.

However, the barrier of the irregularity reduction algorithm [10]-[21] commonly eradicates only irregularity information but also fine information thereupon the main objective of irregularity reduction algorithm is to reduce only irregularity information whereas retain fine information because irregularity information is severely impact on the quality of the digital depictions in the deteriorated manner. By ordinary, the impulse irregularity is destroyed in digital depictions by deterioration machinery as an outcome of depiction keeping proceeding, distribution proceeding, computerized flare or etc. From logical opinion, the impulse irregularity component [22]-[26] may be identified into 2 classes: random magnitude impulse outlier (RMIO) and fix magnitude impulse outlier (FMIO). The RMIO may be any magnitude over the dynamic magnitude, which is varied from "0" to "255" thereupon the RMIO may be more difficultly identified than FMIO where the FMIO may completely be "0" or "255" while the FMIO may be promptly identified than RMIO. The primary restriction of the irregularity identification is to extricate the irregular pixels from the regular pixels, which can be located in either in both steady territory (whereas the adjacent pixels are closely identical) or discontinuous territory (whereas the adjacent pixels are highly diverse). For natural depictions, the generous allotment of depiction pixels is steady territory nonetheless the diminutive allotment is discontinuous territory. Accordingly, in the early years, most irregularity reduction algorithms [22]-[26] were offered for reducing the outlier depiction from impulsive irregularity.

In 1975, the classical median filter (SMF) [10] was formulated for FMIO and, next, has been proceeded to be one of the practical irregularity reduction algorithm. For reducing FMIO on color digital depictions, the vector median filter (VMF) [11] that was proceeded from classical SMF was formulated in 1990 and has been proceeded to be one of the most practical irregularity reduction algorithms for color digital depictions. Subsequently, an adaptive median filter (AMF) [12] that was proceeded from classical SMF where the processed window is automatically adjusted was formulated for FMIO in 1994 and, next, has been proceeded to be one of the most practical irregularity reduction algorithms with exceptional achievement. In 2017, The irregularity reduction algorithm [13] built on intensity conserving cast elimination with swarm optimization was formulated for engaging on color digital depictions. Thereupon, an alternative irregularity reduction algorithm [14] built on self-regulating computer-abetment investigation scheme with support-vector machines (SVM) scheme for engaging on magnetic resonance imaging (MRI) brain digital depictions was formulated in 2017. Succeeding, an irregularity reduction algorithm [15] built on irregularity consistency classification by neighborhood statistic scheme was formulated in 2018. In 2018, an irregularity reduction algorithm [16] built on an efficient filtering scheme was formulated for engaging on color digital depictions. Later, an irregularity reduction algorithm built on the Gaussian filtering and Wiener filtering [17] was studied its achievement by adjusting kernel dimension in 2019. Next, an irregularity reduction algorithm [18] built on filter scheme with MMG technique been formulated for engaging on medical digital depictions in 2019. Charmouti *et al*. [19] studies enormous irregularity reduction algorithm built on various schemes and comparatively simulates these achievements on irregularity reduction perspective in 2019. In 2020, another irregularity reduction algorithm built on a divided wavelet scheme [20] that is proceeded from classic Haar wavelet as divided order using a universal lowpass classification with the divided delay procedure was formulated. For reducing submerged water acoustic irregularity, an irregularity reduction algorithm [21] built on DWT and irregularity frequency evaluation was formulated in 2020.

Today, Enormous contemporary irregularity reduction algorithms [22]-[25] that are ordinarily composed of irregularity identification scheme and irregularity enhancement scheme, are formulated as succeeding. In 2017, the irregularity reduction algorithm [22] built on hybrid stochastic scheme is formulated for engaging on FMIO. For dense frequency of FMIO, alternative irregularity reduction algorithm, so called adaptive decision based inverse distance weighted interpolation (DBIDWI) scheme [23]-[24] that was initially formulated for by Patanavijit [23] in 2017 is studied this performance [24] on almost frequency of FMIO in 2019. Due to enormous irregularity reduction algorithms usually built on rank order absolute difference (ROAD), rank order logarithm difference (ROLD) and rank order relative difference RORD), the comparatively simulations [25] of irregularity reduction algorithms on almost frequency of FMIO was studied in 2019. Next, the irregularity reduction algorithm built on the a two-stage scheme [26] that is derived from the stochastic scheme and this algorithm grants exceptional achievement was formulated for engaging on RMIO in 2020. However, the irregularity reduction algorithm built on the two-stage scheme [26] was never employed on FMIO therefore this paper centralizes on the irregularity reduction algorithm built on the two-stage scheme for FMIO at almost frequency.

2. THE THEORY OF PIXEL SIMILARITY

2.1. Pixel similarity identification

One of the most practical pixel similarity identifications is the absolute difference [26] of the intensity of each pixel in the computed window. If the absolute difference of pixel intensity is great value then the computed pixel is identified as an irregularity pixel but If the absolute difference of pixel intensity is low value then the computed pixel is identified as a regularity pixel. The absolute difference of pixel intensity shall be designated as (1).

$$I_{AB}(x, y) = \left\| G_x - G_y \right\| \tag{1}$$

Where G_x and G_y designates the magnitude of the pixel x and y respectively.

2.2. Pixel similarity identification based on spatial distance

One of the classical pixel similarity identifications is spatial distance, which is first implement on the classical smooth filter where the main idea is that the closer pixel has higher impact than the greater spatial distance. The spatial distance of pixel shall be designated as (2).

$$D_{SPATIAL}(x, y) = \left\| \overline{(m, n)} - \overline{(s, t)} \right\|, y \in \Omega_x^0 \tag{2}$$

Where (s, t) designates the location of the considered pixel x and (m, n) represents the coordinate of any pixel y in window dimension Ω_x^0.

3. THE PROPOSED ALGORITHM

This paper proposes the alternative irregularity reduction algorithm. The irregularity reduction algorithm built on the a two-stage scheme grants exceptional achievement was formulated for engaging on RMIO but the irregularity reduction algorithm built on the two-stage scheme [26] was never employed on FMIO. As a results, the fix magnitude impulse outliers are first noticed by the two-stage scheme, which is comprehensively demonstrated in section 3.1. Later, all noticed impulse outliers are reduced by AMF, which is comprehensively demonstrated in section 3.2.

3.1. The two-stage scheme for irregularity notification

For 5×5 window dimension (Ω_x^0), the identification $S(x, y)$ between the considered pixel x and all pixels y in Ω_x^0, shall be designated as (3) to (5).

$$D(x, y) = \exp\left(\left\| \overline{(m, n)} - \overline{(s, t)} \right\|^2 / 2\sigma_D^2 \right), y \in \Omega_x^0 \tag{3}$$

$$I(x, y) = \exp\left(\left\| G_x - G_y \right\|^2 / 2\sigma_I^2 \right) \tag{4}$$

$$S(x, y) = D(x, y). I(x, y) \tag{5}$$

Where $D(x, y)$ is geometric range between pixels x and y in Gaussian operation and $I(x, y)$ are magnitude range between pixels x and y in Gaussian operation. The entity of the identification between a considered pixel x and all pixel y in window dimension Ω_x^0 shall be designated as (6).

$$\zeta x = \sum_{y \in \Omega_x^0} S(x, y) = \sum_{y \in \Omega_x^0} D(x, y). I(x, y) \tag{6}$$

The novel identification shall be designated as (7).

$$\overline{\zeta x} = \zeta x / \overline{\left(\sum_{y \in \Omega_x^0} \zeta y \right)} \tag{7}$$

Where $\overline{\left(\sum_{y \in \Omega_x^0} \zeta y \right)}$ is the mean of $\sum_{x \in \Omega_x^0} \zeta y$. The normalized novel identification shall be designated as (8).

$$LS_x = \begin{cases} 1 & , \overline{\zeta x} > 2.5 \\ \overline{\zeta x} / 2.5 & , \overline{\zeta x} \leq 2.5 \end{cases} \tag{8}$$

Where LS_x designates the neighborhood identification between a considered pixel x and all pixel y in window dimension Ω_x^0, which shall imply the expectation of whether the pixel x is irregularity or the pixel x is regularity. From this mathematical perception, if the LS_x is great then the pixel x is similar to the pixel x but if the LS_x is lessen then the pixel x is differ to the pixel x.

This piece of the intellectual paper offers the comprehensive process case of the 2-stage identification. The computation of the 2-stage identification is depicted in Figure 1. The first case shows that the considered pixel $x(i,j) = 0$ is irregularity and this pixel is identified as irregularity in Figure 1(a) where the red color pixels are irregularity. The second case shows that the considered pixel is regularity and this pixel is identified as regularity in Figure 1(b) where the red color pixels are irregularity.

3.2. The adaptive median filter for irregularity reduction

If normalized novel identification LS_x great then the irregularity threshold then a considered pixel shall be a irregularity. Therefore, the irregularity pixel shall be reduced the outlier by AMF operation [12]. Otherwise, if normalized novel identification LS_x lessen then the irregularity threshold then a considered pixel shall be a regularity.

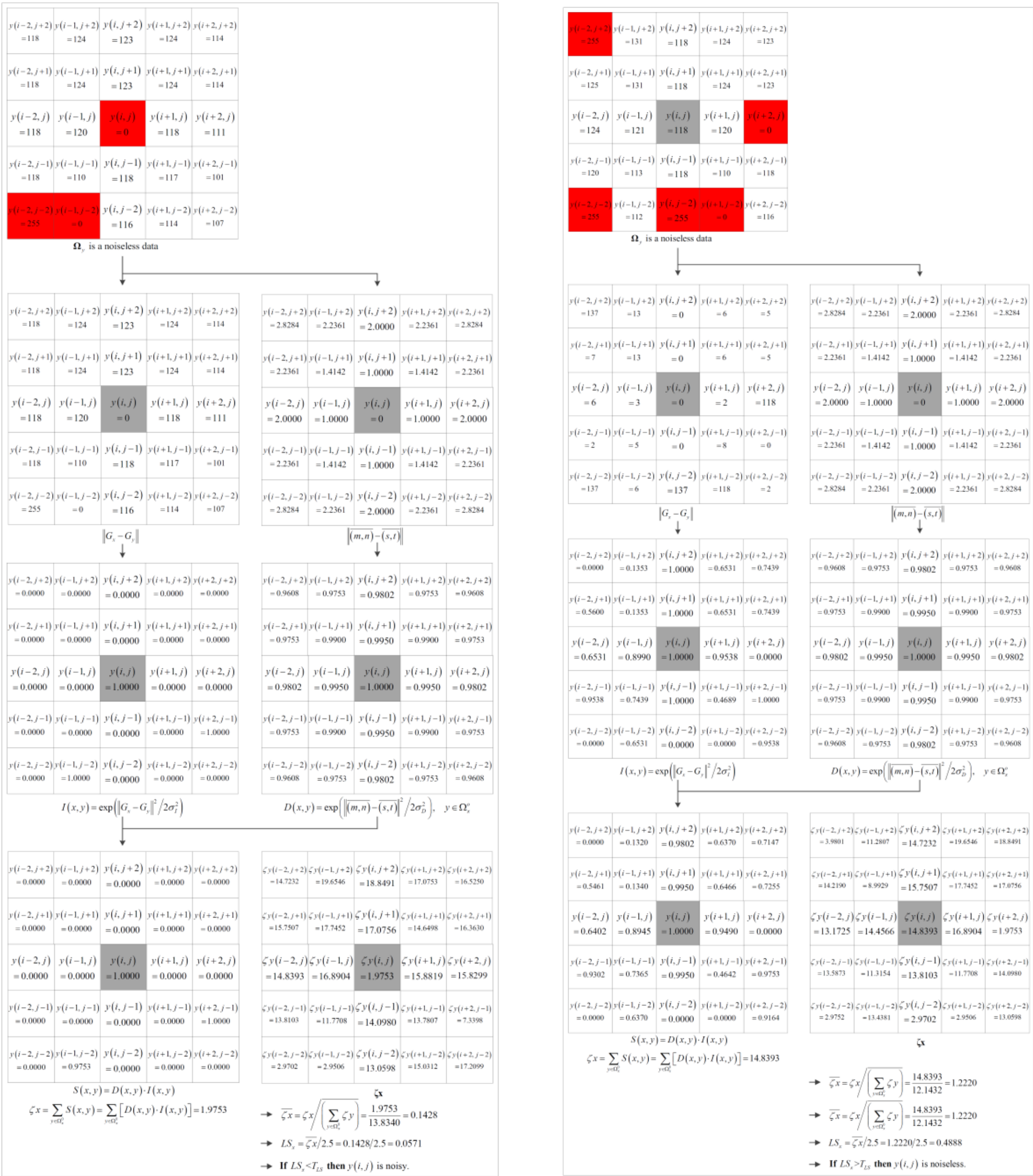

(a) (b)

Figure 1. The comprehensive process case of the 2-stage identification (a) the x is irregularity ($x(i,j) = 0$) and (b) the x is regularity ($x(i,j) = 118$)

4. RESULTS AND DISCUSSION

For this piece of the intellectual paper, the MATLAB is the program for these experimental simulations. This MATLAB are installed and implemented under prolific computers with hardware structure: Main Processor i7-6700HQ and main memory 16 GB. Each computer implements on these prolific digital depictions in each following experimental cases.

4.1. The experimental simulation of the optimized window dimension for 2-stage scheme

The first experiment aims attention at the stochastic characteristic relationship (the expectation and the SD) between 2-Stage identification and the window dimension of regularity and irregularity pixels. This experiment is implemented on Lena, Girl and Pepper under FMIO at little, mild and immense massiveness (from 5% to 90%) as shown in Figure 2. The experimental result of Lena (3x3,5x5,7x7,9x9), Girl (3x3,5x5,7x7,9x9) and Pepper (3x3,5x5,7x7,9x9) is depicted in Figure 2(a) to Figure 2(c), respectively.

From the first experiment results of Lena, Girl and Pepper, when the window dimension of 2-Stage identification is increased, the expectation of irregularity pixels is decreased and the expectation of regularity pixels is increased for FMIO at range about 5%-55% to 5%-70% therefore the impulsive outlier can effectively identify whether the considered pixel is identified as regularity or irregularity. However, when the window dimension of 2-Stage identification is increased from 3x3 to 9x9, the intersection between the expectation of irregularity pixels and regularity pixels is reduce from 5%-70% to 5%-60%. In the physical sense, if the window dimension is 3x3 then the 2-Stage identification can identify the impulsive outlier at range about 5%-70% but if the window dimension is 9x9 then the 2-Stage identification can identify the impulsive outlier at range about 5%-60%. From the computation complexity, the identification range, the accuracy point of view, the window dimension is set to be 5x5 for producing the optimized performance at range about 5%-70%.

4.2. The experimental simulation of the irregularity truthfulness for 2-stage scheme

The second experiment of the 2-state truthfulness is simulated for engaging on FMIO at at little, mild and immense massiveness (5% to 90%) on Lena, Girl and Pepper in Table 1 to Table 3, respectively. First, the irregularity truthfulness experiments of 2-state scheme on Lena, Girl and Pepper are depicted in Table 1(a), Table 2(a) and Table 3(a), respectively. Later, the regularity truthfulness experiments of 2-state scheme on Lena, Girl, F16 and Pepper are depicted in Table 1(b), Table 2(b) and Table 3(b), respectively. From these results, the irregularity truthfulness increases when the irregularity threshold increases but the regularity truthfulness increases when the irregularity threshold decreases.

4.3. The experimental simulation of the optimized 2-stage constant for alternative irregularity reduction algorithm built on 2-stage scheme

This section presents the third experiment results. The interrelationship between the overall outlier reduction efficacy of a proposed irregularity reduction algorithm (built on 2-stage and AMF) and the 2-Stage constant are examined for Lena, Girl and Pepper under FMIO as depicted in Table 4 to Table 6, respectively. For FMIO at range about 5%-90%, the optimal 2-Stage constant, which produces the maximum efficacy (PSNR), must be 0.45-0.50.

4.4. The experimental simulation of the performance of alternative irregularity reduction algorithm

This section presents the last experiment results. The efficacy of the 2-stage outlier reduction algorithm built on 2-stage and AMF (at 1^{st} iteration and N^{th} iteration) is comparatively examined with other up-to-the-minute outlier reduction algorithms such as MF (Mean Filter), SMF (Standard Median Filter) and AMF. The interrelationship between the efficacy in PSNR (the 2-Stage outlier reduction and other up-to-the-minute outlier reductions) and outlier massiveness of Lena, Girl and Pepper are depicted in Table 7 - Table 9.

From these experiment results of Lena in Table 7, the performance of the proposed irregularity reduction is noticeably greater than MF [1], SMF [10] and AMF [12] about 13.6391±1.9048 dB, 9.2847±3.4503 dB and 3.5747±2.1803 dB, respectively. From these experiment results of Girl in Table 8, the performance of the proposed irregularity reduction is noticeably greater than MF, SMF and AMF about 19.2145±0.3013 dB, 13.8584±5.0997 dB and 6.0999±3.6961 dB, respectively. From these experiment results of Pepper in Table 9, the performance of the proposed irregularity reduction is noticeably greater than MF, SMF and AMF about 13.6914±2.4551 dB, 9.4333±2.7953 dB and 3.3399±2.1160 dB, respectively. From these experiment results (in Table 7 to Table 9), the outlier reduced images from the 2-Stage outlier reduction built on 2-stage scheme and AMF (N^{th} iteration) have the highest efficacy than the outlier reduced images from other outlier reduction (such as MF, SMF and AMF). For visualization perspective, the outlier reduced results of the depictions (Lena), which are computed by the proposed irregularity reduction algorithm and compared with other up-to-the-minute outlier reduction algorithms such as MF (Mean Filter), SMF (Standard Median Filter) and AMF, are depicted in Figure 3.

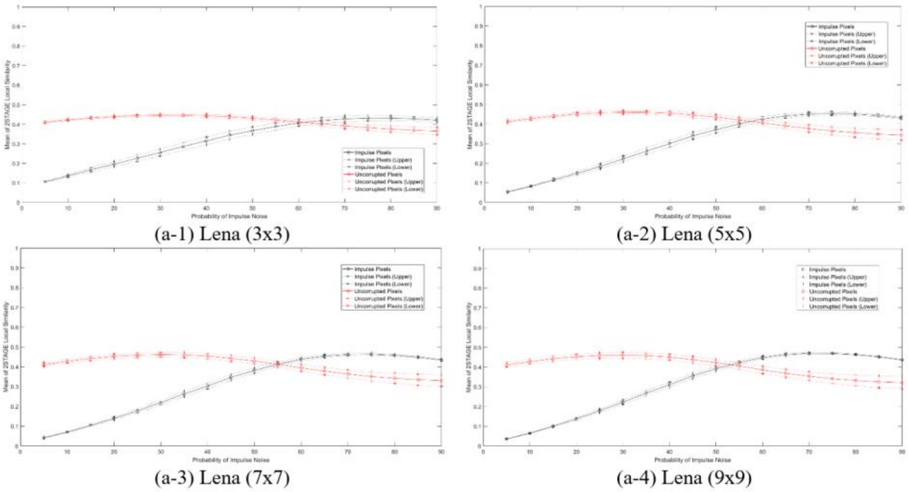

(a-1) Lena (3x3) (a-2) Lena (5x5)

(a-3) Lena (7x7) (a-4) Lena (9x9)

(a)

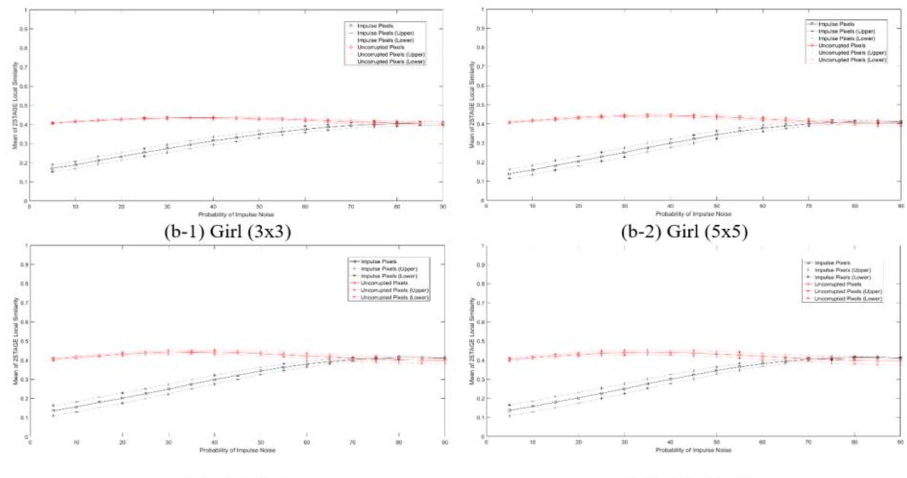

(b-1) Girl (3x3) (b-2) Girl (5x5)

(b-3) Girl (7x7) (b-4) Girl (9x9)

(b)

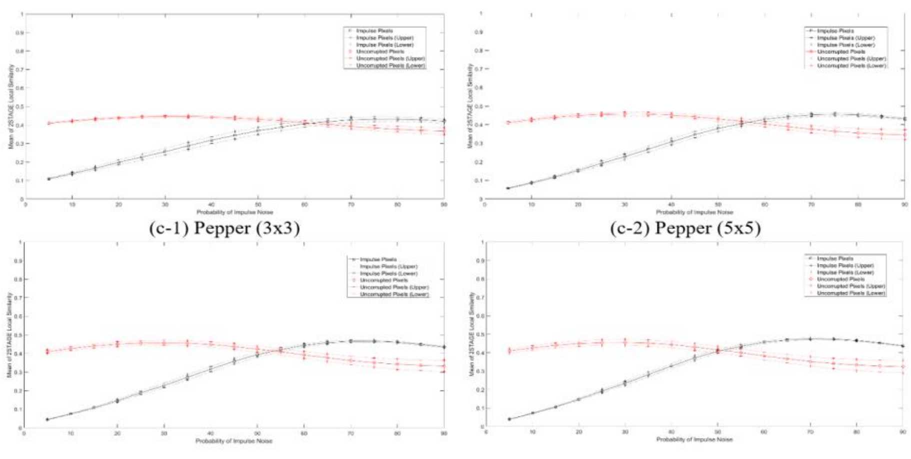

(c-1) Pepper (3x3) (c-2) Pepper (5x5)

(c-3) Pepper (7x7) (c-4) Pepper (9x9)

(c)

Figure 2. The comprehensive process case of the 2-stage identification (a) Lena, (b) Girl, and (c) Pepper

Table 1. 2-stage scheme Lena of (a) irregularity truthfulness and (b) regularity truthfulness

(a)

2-S	Irregularity truthfulness (%)																	
Cons.	5	10	15	20	25	30	35	40	45	50	55	60	65	70	75	80	85	90
0.05	51.87	27.25	13.53	6.47	3.19	1.54	0.71	0.32	0.14	0.07	0.03	0.01	0.01	0.00	0.00	0.00	0.00	0.00
0.10	0.01	71.71	50.45	31.52	17.93	9.81	4.89	2.51	1.21	0.57	0.28	0.11	0.06	0.03	0.02	0.01	0.01	0.01
0.15	0.08	88.99	75.85	58.44	40.82	26.75	15.54	8.94	4.63	2.41	1.27	0.60	0.33	0.19	0.15	0.09	0.09	0.08
0.20	0.50	95.77	88.87	76.76	61.80	46.18	31.45	20.41	12.04	6.83	3.90	2.21	1.34	0.85	0.69	0.53	0.50	0.50
0.25	2.03	98.06	94.56	87.51	77.07	63.62	48.95	35.21	23.52	14.76	9.42	5.86	3.88	2.69	2.24	1.98	1.96	2.03
0.30	6.32	99.13	97.17	93.23	86.72	76.90	64.49	51.26	37.98	26.68	18.56	12.88	9.15	6.89	6.00	5.56	5.82	6.32
0.35	15.63	99.66	98.60	96.36	92.41	85.81	76.92	66.11	53.52	41.44	31.50	23.85	18.43	14.93	13.46	12.95	13.97	15.63
0.40	31.79	99.85	99.27	98.13	95.71	91.64	85.78	78.05	68.17	57.17	47.13	38.53	32.02	27.58	25.80	25.98	28.12	31.79
0.45	54.80	99.94	99.66	99.04	97.69	95.23	91.69	86.62	79.84	71.63	63.25	55.46	49.29	45.05	43.58	44.78	48.46	54.80

(b)

2-S	Regularity truthfulness (%)																	
Cons.	5	10	15	20	25	30	35	40	45	50	55	60	65	70	75	80	85	90
0.05	99.92	99.94	99.96	99.97	99.97	99.98	99.99	99.99	100.0	100.0	100.0	99.97	99.89	99.61	98.75	96.74	92.04	81.40
0.10	42.29	99.49	99.53	99.56	99.60	99.59	99.55	99.45	99.30	99.05	98.62	97.94	96.62	94.17	89.69	81.22	65.88	42.29
0.15	15.98	98.61	98.72	98.74	98.82	98.72	98.57	98.38	97.92	97.18	95.98	94.01	90.56	84.32	74.53	59.12	37.91	15.98
0.20	5.08	97.09	97.28	97.39	97.40	97.35	96.99	96.48	95.59	94.10	91.72	87.72	81.57	70.50	55.82	37.24	18.46	5.08
0.25	1.43	94.52	94.97	95.20	95.25	95.13	94.51	93.67	92.00	89.47	85.50	79.04	69.42	54.37	37.29	20.82	7.88	1.43
0.30	0.35	90.42	91.33	91.83	92.00	91.74	90.98	89.56	87.01	82.92	76.65	67.31	54.69	38.07	22.21	10.15	3.04	0.35
0.35	0.10	83.90	85.56	86.63	87.14	86.72	85.71	83.69	79.74	73.67	65.01	53.15	39.13	23.71	11.74	4.20	0.99	0.10
0.40	0.01	72.63	76.13	78.40	79.44	79.36	77.89	74.94	69.65	61.32	50.73	37.57	24.68	12.81	5.28	1.60	0.31	0.01
0.45	0.00	51.55	59.56	64.48	67.10	67.49	66.08	61.96	55.17	45.49	34.65	23.17	13.42	5.84	1.92	0.48	0.10	0.00

Table 2. 2-stage scheme (Girl) of (a) irregularity truthfulness and (b) regularity truthfulness

(a)

2-S	Irregularity truthfulness (%)																	
Cons.	5	10	15	20	25	30	35	40	45	50	55	60	65	70	75	80	85	90
0.05	52.53	35.32	22.06	12.54	6.94	3.78	2.07	1.08	0.52	0.27	0.13	0.07	0.02	0.01	0.00	0.00	0.00	0.00
0.10	0.01	61.49	50.88	39.50	28.61	20.10	13.09	8.40	5.05	3.01	1.83	0.98	0.46	0.28	0.13	0.05	0.03	0.01
0.15	0.16	70.55	64.44	56.98	47.45	37.73	28.55	20.86	14.29	9.33	6.28	4.00	2.35	1.40	0.85	0.48	0.27	0.16
0.20	0.99	74.46	71.06	66.14	59.64	51.82	44.10	36.06	28.19	21.24	16.12	11.83	8.01	5.43	3.77	2.34	1.48	0.99
0.25	3.73	77.14	74.64	71.40	66.91	61.16	54.99	47.88	40.17	32.79	26.58	21.14	16.28	12.12	9.42	6.80	5.00	3.73
0.30	10.12	79.30	77.51	75.13	71.81	67.63	62.86	57.32	50.77	43.94	37.72	31.95	26.77	21.70	18.19	14.74	11.98	10.12
0.35	22.79	81.67	80.31	78.17	75.61	72.62	68.82	64.62	59.47	53.62	48.20	43.18	38.38	33.64	30.25	27.16	24.55	22.79
0.40	42.02	85.68	83.94	81.59	79.52	76.98	73.91	70.75	66.87	62.20	57.75	53.63	49.89	46.36	44.03	42.70	41.86	42.02
0.45	66.29	97.61	96.15	93.65	90.50	86.88	82.81	79.25	75.53	71.81	68.52	65.76	63.44	61.92	61.06	61.96	63.59	66.29

(b)

2-S	Regularity truthfulness (%)																	
Cons.	5	10	15	20	25	30	35	40	45	50	55	60	65	70	75	80	85	90
0.05	99.98	99.98	99.98	99.98	99.98	99.98	99.97	99.97	99.96	99.94	99.93	99.86	99.81	99.64	99.40	98.93	98.17	96.95
0.10	91.34	99.75	99.75	99.73	99.69	99.68	99.65	99.60	99.45	99.29	99.10	98.78	98.30	97.61	96.52	94.98	93.15	91.34
0.15	87.08	99.21	99.21	99.17	99.09	99.06	98.92	98.76	98.49	98.06	97.55	96.89	95.78	94.32	92.43	90.01	87.90	87.08
0.20	84.19	98.24	98.27	98.22	98.15	98.06	97.76	97.47	96.99	96.33	95.42	94.40	92.69	90.42	87.80	85.04	83.42	84.19
0.25	81.88	96.66	96.82	96.80	96.73	96.51	96.15	95.71	94.95	94.04	92.80	91.20	88.80	85.94	82.74	80.52	79.71	81.88
0.30	78.43	94.42	94.72	94.77	94.74	94.50	94.00	93.37	92.36	91.03	89.42	87.23	84.24	80.95	77.69	76.16	76.01	78.43
0.35	71.11	90.89	91.49	91.76	91.80	91.55	91.08	90.25	88.95	87.17	85.05	82.16	78.73	75.06	72.18	70.79	70.03	71.11
0.40	56.47	82.40	84.77	86.19	86.88	86.92	86.58	85.66	83.96	81.65	78.68	75.16	70.89	66.55	63.51	61.14	58.18	56.47
0.45	32.27	21.97	32.56	43.20	52.71	60.90	66.95	69.82	70.31	68.09	64.19	59.64	54.42	48.91	45.04	40.76	36.32	32.27

Table 3. 2-stage scheme (Pepper) of (a) irregularity truthfulness and (b) regularity truthfulness

(a)

2-S	Irregularity truthfulness (%)																	
Cons.	5	10	15	20	25	30	35	40	45	50	55	60	65	70	75	80	85	90
0.05	64.00	37.37	19.43	8.99	3.96	1.86	0.78	0.38	0.17	0.08	0.03	0.01	0.01	0.00	0.00	0.00	0.00	0.00
0.10	0.01	77.30	58.78	39.74	24.32	14.11	6.89	3.37	1.51	0.70	0.34	0.16	0.07	0.03	0.02	0.01	0.01	0.01
0.15	0.08	91.80	81.24	66.47	49.22	34.14	20.82	12.14	6.43	3.29	1.68	0.83	0.43	0.23	0.16	0.10	0.09	0.08
0.20	0.50	96.52	91.13	81.81	69.46	54.37	39.23	26.29	16.18	9.31	5.28	2.94	1.74	1.02	0.75	0.57	0.51	0.50
0.25	2.05	98.37	95.47	90.41	82.24	70.43	57.04	43.17	29.90	19.34	12.44	7.82	4.91	3.24	2.53	2.10	2.02	2.05
0.30	6.40	99.26	97.67	94.75	89.92	81.71	71.67	59.34	45.92	33.06	23.46	16.42	11.30	8.15	6.71	5.88	6.01	6.40
0.35	15.83	99.63	98.85	97.15	94.41	89.08	82.19	72.92	61.42	48.78	37.90	29.06	21.83	17.12	14.72	13.73	14.39	15.83
0.40	32.08	99.83	99.36	98.46	96.94	93.65	89.27	83.04	74.51	64.24	54.02	44.50	36.61	31.00	27.98	27.28	28.80	32.08
0.45	55.26	99.91	99.68	99.14	98.32	96.40	93.73	89.84	84.37	77.14	69.53	61.53	54.49	49.21	46.46	46.67	49.55	55.26

(b)

2-S	Regularity truthfulness (%)																	
Cons.	5	10	15	20	25	30	35	40	45	50	55	60	65	70	75	80	85	90
0.05	99.97	99.98	99.99	99.99	99.99	100.0	100.0	100.0	100.0	100.0	99.99	99.98	99.93	99.67	99.05	97.54	93.70	84.54
0.10	49.48	99.68	99.72	99.72	99.74	99.71	99.68	99.61	99.52	99.27	99.03	98.49	97.51	95.81	92.26	85.61	72.11	49.48
0.15	21.36	99.19	99.24	99.25	99.22	99.20	99.08	98.88	98.52	98.01	97.18	95.68	93.00	88.45	80.41	66.68	45.78	21.36
0.20	7.75	98.34	98.43	98.44	98.43	98.28	98.10	97.65	96.89	95.89	94.11	91.22	86.03	77.34	64.01	45.65	24.48	7.75
0.25	2.52	96.85	97.07	97.13	97.15	96.86	96.53	95.78	94.52	92.71	89.58	84.50	76.07	63.13	46.34	27.70	11.45	2.52
0.30	0.68	94.30	94.85	95.02	95.12	94.71	94.12	93.03	91.04	88.03	82.95	75.09	63.22	47.21	29.66	14.52	4.83	0.68
0.35	0.22	89.76	90.99	91.58	91.80	91.46	90.56	88.94	85.88	81.02	73.29	62.55	48.16	31.51	16.95	6.66	1.79	0.22
0.40	0.06	79.25	83.13	85.32	86.15	86.12	84.88	82.47	77.93	70.41	60.18	47.31	32.28	18.21	8.21	2.64	0.60	0.06
0.45	0.03	40.11	57.51	68.53	73.88	75.43	74.44	70.99	64.48	54.67	43.21	30.52	18.36	8.88	3.32	0.82	0.18	0.03

Table 4. Stochastic characteristic relationship between PSNR and 2-Stage constant of LENA image (FMIO)

2-S	PSNR (dB)																	
Cons.	5	10	15	20	25	30	35	40	45	50	55	60	65	70	75	80	85	90
0.025	19.92	16.09	13.97	12.68	11.69	10.90	10.22	9.65	9.07	8.66	8.21	7.78	7.49	7.17	6.85	6.58	6.32	6.06
0.050	22.76	17.46	14.60	12.99	11.84	10.97	10.26	9.66	9.08	8.66	8.21	7.78	7.49	7.17	6.84	6.56	6.29	6.01
0.075	25.58	19.16	15.69	13.65	12.25	11.17	10.36	9.71	9.09	8.66	8.21	7.77	7.48	7.15	6.81	6.53	6.24	5.94
0.100	28.34	21.17	17.07	14.54	12.81	11.46	10.52	9.79	9.13	8.68	8.22	7.77	7.47	7.13	6.78	6.49	6.19	5.91
0.125	30.59	23.04	18.50	15.61	13.48	11.91	10.80	9.95	9.20	8.71	8.22	7.76	7.46	7.11	6.74	6.45	6.13	5.87
0.150	32.31	24.89	19.96	16.79	14.31	12.51	11.17	10.15	9.30	8.77	8.25	7.77	7.45	7.08	6.71	6.41	6.10	5.85
0.175	34.12	26.58	21.43	18.05	15.19	13.20	11.60	10.45	9.47	8.86	8.29	7.78	7.44	7.06	6.67	6.38	6.07	5.84
0.200	35.41	28.32	22.78	19.19	16.17	13.95	12.13	10.80	9.69	9.02	8.37	7.81	7.46	7.05	6.65	6.35	6.06	5.84
0.225	36.59	29.84	24.06	20.30	17.14	14.83	12.77	11.26	9.98	9.21	8.47	7.85	7.47	7.04	6.63	6.35	6.07	5.86
0.250	36.73	31.63	25.35	21.53	18.21	15.74	13.39	11.77	10.34	9.45	8.62	7.95	7.52	7.07	6.64	6.36	6.10	5.90
0.275	37.14	32.80	26.62	22.58	19.28	16.61	14.16	12.38	10.77	9.75	8.82	8.06	7.58	7.11	6.68	6.40	6.16	5.96
0.300	**37.17**	34.04	27.80	23.63	20.28	17.53	15.01	13.00	11.28	10.13	9.09	8.25	7.71	7.20	6.77	6.48	6.25	6.07
0.325	37.12	34.43	28.54	24.74	21.33	18.44	15.84	13.73	11.85	10.58	9.41	8.45	7.87	7.35	6.89	6.60	6.40	6.24
0.350	36.86	35.00	29.68	25.74	22.33	19.44	16.69	14.50	12.46	11.10	9.80	8.73	8.11	7.55	7.08	6.80	6.61	6.47
0.375	36.81	35.42	30.45	26.47	23.17	20.41	17.56	15.32	13.11	11.68	10.25	9.10	8.41	7.82	7.34	7.06	6.90	6.81
0.400	36.57	35.34	31.00	27.38	24.16	21.36	18.38	16.14	13.82	12.31	10.79	9.55	8.82	8.19	7.68	7.43	7.30	7.30
0.425	36.40	35.39	31.57	28.15	25.22	22.21	19.16	17.00	14.54	12.98	11.40	10.10	9.31	8.65	8.15	7.92	7.84	7.97
0.450	36.31	**35.52**	31.99	28.90	25.87	23.01	20.04	17.83	15.26	13.73	12.10	10.75	9.94	9.26	8.73	8.56	8.54	8.86
0.475	36.24	35.43	32.51	29.70	26.56	23.86	20.75	18.61	16.02	14.51	12.89	11.47	10.69	9.97	9.47	9.38	9.49	10.01
0.500	36.19	35.39	**32.94**	**30.10**	**27.10**	**24.36**	**21.43**	**19.41**	**16.79**	**15.32**	**13.75**	**12.31**	**11.58**	**10.89**	**10.40**	**10.41**	**10.71**	**11.50**

Table 5. Stochastic characteristic relationship between PSNR and 2-Stage constant of GIRL image (FMIO)

2-S	PSNR (dB)																	
Cons	5	10	15	20	25	30	35	40	45	50	55	60	65	70	75	80	85	90
0.025	18.17	14.62	12.40	10.87	9.64	8.92	8.12	7.59	7.08	6.57	6.21	5.86	5.48	5.13	4.87	4.57	4.31	4.06
0.050	21.81	16.88	13.67	11.59	10.04	9.17	8.24	7.66	7.11	6.59	6.22	5.87	5.48	5.13	4.86	4.56	4.29	4.04
0.075	25.42	19.48	15.53	12.84	10.78	9.73	8.55	7.87	7.22	6.65	6.25	5.88	5.49	5.13	4.86	4.55	4.28	4.02
0.100	28.98	22.09	17.75	14.29	11.88	10.55	9.07	8.24	7.47	6.79	6.34	5.93	5.51	5.13	4.85	4.53	4.27	4.01
0.125	31.99	24.27	19.80	15.89	13.19	11.49	9.75	8.74	7.83	7.00	6.47	6.01	5.56	5.14	4.85	4.53	4.26	4.00
0.150	33.93	26.23	21.59	17.51	14.40	12.46	10.49	9.32	8.26	7.30	6.70	6.16	5.65	5.18	4.88	4.54	4.26	4.00
0.175	35.84	27.95	23.23	18.99	15.73	13.59	11.49	10.14	8.89	7.80	7.10	6.46	5.84	5.31	4.96	4.58	4.28	4.01
0.200	37.06	29.99	24.74	20.51	17.22	14.92	12.61	11.07	9.69	8.40	7.62	6.84	6.12	5.49	5.09	4.65	4.32	4.04
0.225	37.65	31.35	26.41	22.05	18.69	16.08	13.63	11.94	10.41	9.01	8.09	7.22	6.41	5.70	5.24	4.77	4.40	4.10
0.250	38.44	33.12	28.00	23.30	19.93	17.21	14.65	12.86	11.26	9.71	8.70	7.78	6.85	6.06	5.53	4.97	4.56	4.22
0.275	**38.77**	34.01	29.42	24.45	21.21	18.43	15.68	13.84	12.19	10.58	9.45	8.42	7.36	6.50	5.89	5.23	4.77	4.38
0.300	38.60	34.88	30.43	25.92	22.45	19.52	16.78	14.78	13.07	11.35	10.13	9.02	7.86	6.96	6.28	5.57	5.05	4.61
0.325	38.37	35.11	31.65	26.98	23.65	20.72	17.78	15.69	14.10	12.23	10.90	9.78	8.51	7.55	6.82	6.08	5.47	4.98
0.350	38.29	35.76	32.63	27.99	24.81	21.77	18.74	16.66	15.02	13.14	11.71	10.50	9.21	8.20	7.46	6.62	5.97	5.43
0.375	38.11	35.81	33.45	29.07	25.63	22.92	19.69	17.53	16.01	14.01	12.46	11.19	9.91	8.86	8.11	7.26	6.62	6.04
0.400	37.93	36.05	33.81	29.91	26.84	23.96	20.61	18.37	16.95	14.80	13.30	11.96	10.68	9.62	8.91	8.09	7.50	6.89
0.425	37.75	36.15	34.08	30.24	27.64	24.77	21.25	19.15	17.77	15.49	14.05	12.77	11.49	10.40	9.74	8.99	8.53	7.98
0.450	37.67	36.22	34.05	30.65	27.98	25.16	21.84	19.87	18.48	16.11	14.73	13.51	12.25	11.24	10.66	10.00	9.76	9.29
0.475	37.66	36.41	**34.47**	30.77	28.09	25.65	22.24	20.38	18.92	16.70	15.42	14.19	13.02	12.15	11.64	11.18	11.17	10.90
0.500	37.64	**36.56**	34.35	**30.93**	**28.32**	**25.99**	**22.68**	**20.89**	**19.43**	**17.32**	**16.07**	**14.95**	**13.78**	**13.07**	**12.62**	**12.41**	**12.59**	**12.85**

Table 6. Stochastic characteristic relationship between PSNR and 2-Stage constant of Pepper image (FMIO)

2-S	PSNR (dB)																	
Cons.	5	10	15	20	25	30	35	40	45	50	55	60	65	70	75	80	85	90
0.025	19.40	15.73	13.69	12.39	11.40	10.63	9.97	9.40	8.86	8.38	7.99	7.62	7.27	6.92	6.64	6.37	6.11	5.86
0.050	21.83	17.02	14.30	12.69	11.54	10.69	10.01	9.42	8.86	8.39	7.99	7.62	7.27	6.92	6.63	6.35	6.07	5.80
0.075	24.96	18.78	15.35	13.29	11.88	10.88	10.09	9.45	8.87	8.39	7.99	7.61	7.26	6.90	6.60	6.31	6.02	5.75
0.100	27.52	20.63	16.61	14.05	12.38	11.16	10.24	9.52	8.91	8.40	7.99	7.61	7.24	6.88	6.57	6.27	5.97	5.71
0.125	30.38	22.25	17.96	15.02	13.02	11.58	10.48	9.66	8.97	8.43	8.00	7.60	7.23	6.85	6.53	6.22	5.92	5.67
0.150	32.51	23.85	19.45	16.10	13.79	12.12	10.81	9.86	9.07	8.48	8.03	7.60	7.22	6.82	6.49	6.18	5.88	5.65
0.175	33.97	25.48	20.92	17.26	14.64	12.73	11.26	10.14	9.23	8.56	8.06	7.61	7.21	6.79	6.46	6.15	5.86	5.64
0.200	34.86	26.93	22.29	18.51	15.51	13.42	11.80	10.46	9.45	8.69	8.13	7.65	7.21	6.78	6.43	6.13	5.85	5.64
0.225	37.19	28.42	23.70	19.66	16.43	14.17	12.38	10.89	9.74	8.85	8.23	7.70	7.23	6.78	6.42	6.12	5.86	5.66
0.250	37.43	29.95	24.89	20.75	17.38	14.99	13.04	11.39	10.09	9.07	8.37	7.78	7.28	6.80	6.43	6.14	5.89	5.70
0.275	**37.76**	30.99	26.07	21.91	18.36	15.81	13.76	11.92	10.51	9.35	8.56	7.89	7.34	6.85	6.46	6.18	5.94	5.77
0.300	37.71	32.13	27.27	22.95	19.43	16.76	14.53	12.53	11.00	9.69	8.80	8.07	7.47	6.94	6.53	6.26	6.04	5.88
0.325	37.74	33.24	28.55	24.08	20.50	17.57	15.30	13.17	11.55	10.10	9.11	8.28	7.62	7.07	6.65	6.38	6.18	6.05
0.350	37.64	34.27	29.64	25.13	21.53	18.48	16.13	13.91	12.17	10.56	9.47	8.57	7.86	7.26	6.82	6.56	6.39	6.30
0.375	37.46	34.75	30.49	26.25	22.58	19.43	16.99	14.67	12.80	11.09	9.90	8.91	8.15	7.53	7.06	6.81	6.68	6.66
0.400	37.32	35.28	31.26	27.30	23.57	20.35	17.82	15.46	13.49	11.71	10.42	9.37	8.55	7.86	7.41	7.16	7.07	7.14
0.425	37.20	35.54	31.69	28.01	24.53	21.31	18.68	16.29	14.16	12.33	11.00	9.87	9.00	8.30	7.85	7.62	7.59	7.81
0.450	37.24	35.71	32.46	28.88	25.42	22.10	19.52	17.12	14.90	13.05	11.69	10.50	9.58	8.86	8.46	8.25	8.30	8.69
0.475	37.21	35.74	32.79	29.85	26.11	22.78	20.36	17.95	15.66	13.87	12.45	11.21	10.29	9.56	9.21	9.05	9.24	9.83
0.500	37.18	**35.81**	**32.95**	**30.29**	**26.86**	**23.47**	**21.13**	**18.77**	**16.39**	**14.71**	**13.29**	**12.05**	**11.13**	**10.42**	**10.19**	**10.05**	**10.42**	**11.30**

Table 7. Stochastic characteristic relationship between PSNR and 2-Stage constant of Lena image (FMIO)

Simulated images	Irregularity frequency (%)	Outlie red image	PSNR (dB) Irregularity reduction algorithm				
			MF (3x3)	SMF (3x3)	AMF	2S-AMF-1	2S-AMF-N
Lena (256x256)	D=5	18.7139	22.4181	31.6421	36.0907	37.1720	**37.1720**
	D=10	15.6564	19.3812	30.7076	35.3032	35.5151	**35.5151**
	D=15	13.8274	17.5385	29.2982	33.7454	32.9371	**32.7536**
	D=20	12.6389	16.3208	27.6257	32.1558	30.0969	**32.0436**
	D=25	11.6783	15.3526	25.4101	29.8105	27.0975	**30.7821**
	D=30	10.8971	14.5829	23.6811	27.9141	24.3596	**29.7181**
	D=35	10.2240	13.8785	20.8127	25.6654	21.4251	**28.7420**
	D=40	9.6481	13.2479	19.0080	23.7903	19.4061	**28.0992**
	D=45	9.0745	12.6598	16.8389	21.5949	16.7937	**27.1276**
	D=50	8.6553	12.2146	15.4758	20.5725	15.3180	**26.8051**
	D=55	8.2118	11.7609	13.8573	19.4896	13.7489	**25.5509**
	D=60	7.7813	11.2939	12.3280	18.1747	12.3119	**24.2432**
	D=65	7.4884	11.0012	11.3251	17.7283	11.5796	**23.7380**
	D=70	7.1697	10.6509	10.2861	17.1153	10.8934	**22.1734**
	D=75	6.8497	10.2599	9.1271	16.5388	10.4031	**21.3091**
	D=80	6.5846	10.0057	8.3331	16.4554	10.4123	**21.0006**
	D=85	6.3241	9.7338	7.5344	16.4230	10.7090	**20.3536**
	D=90	6.0604	9.4356	6.8241	16.5352	11.5020	**20.1126**

Table 8. Stochastic characteristic relationship between PSNR and 2-Stage constant of Girl image (FMIO)

Simulated images	Irregularity frequency (%)	Outlie red image	PSNR (dB) Irregularity reduction algorithm				
			MF (3x3)	SMF (3x3)	AMF	2S-AMF-1	2S-AMF-N
Girl (256x256)	D=5	16.4490	20.0454	32.4867	37.5518	38.7659	**38.7659**
	D=10	13.6890	17.2530	31.5583	36.8900	36.5586	**36.5586**
	D=15	11.9287	15.3515	27.6179	34.8060	34.4744	**34.4744**
	D=20	10.6567	13.9593	25.5153	32.0377	30.9324	**33.1956**
	D=25	9.5498	12.7248	22.9614	29.6044	28.3177	**32.6259**
	D=30	8.8677	11.9599	20.7738	27.6911	25.9859	**31.5132**
	D=35	8.0984	11.0501	18.4410	24.9701	22.6771	**30.6277**
	D=40	7.5798	10.4543	16.5146	23.3733	20.8940	**29.9449**
	D=45	7.0728	9.8471	14.8145	21.8116	19.4285	**28.9919**
	D=50	6.5712	9.2367	13.0319	20.1711	17.3236	**28.5322**
	D=55	6.2085	8.7895	11.8226	19.2184	16.0677	**27.9970**
	D=60	5.8609	8.3590	10.4981	18.4518	14.9533	**27.2772**
	D=65	5.4832	7.8712	9.1396	17.2740	13.7838	**27.0087**
	D=70	5.1311	7.4271	8.0463	16.7334	13.0681	**26.7265**
	D=75	4.8712	7.0814	7.1994	16.2921	12.6203	**26.4142**
	D=80	4.5674	6.6881	6.2520	16.2795	12.4098	**25.6450**
	D=85	4.3054	6.3340	5.4218	16.5924	12.5936	**25.1655**
	D=90	4.0573	5.9986	4.7465	16.7463	12.8463	**24.8283**

Table 9. Stochastic characteristic relationship between PSNR and 2-Stage constant of Pepper image (FMIO)

Simulated images	Irregularity frequency (%)	Outlie red image	PSNR (dB) Irregularity reduction algorithm				
			MF (3x3)	SMF (3x3)	AMF	2S-AMF-1	2S-AMF-N
Pepper (256x256)	D=5	18.4752	22.1408	32.2578	37.1145	37.7554	**37.7554**
	D=10	15.3798	19.0677	30.6116	36.0391	35.8119	**35.8119**
	D=15	13.5570	17.2234	28.8470	33.6095	32.9473	**33.3176**
	D=20	12.3593	15.9804	26.5888	31.6485	30.2886	**32.0527**
	D=25	11.3929	14.9986	24.2073	29.4205	26.8626	**31.0632**
	D=30	10.6242	14.1748	22.0663	26.7650	23.4681	**30.0679**
	D=35	9.9742	13.5209	20.3774	25.5249	21.1324	**28.7102**
	D=40	9.3998	12.9076	18.4321	23.4995	18.7697	**28.7102**
	D=45	8.8599	12.3275	16.6168	21.7177	16.3870	**26.9228**
	D=50	8.3843	11.8117	14.8506	20.2203	14.7130	**25.9491**
	D=55	7.9930	11.3720	13.4655	19.0894	13.2941	**25.1464**
	D=60	7.6189	10.9563	12.0128	18.1116	12.0459	**23.4968**
	D=65	7.2684	10.5758	10.8920	17.3657	11.1284	**22.4737**
	D=70	6.9246	10.2039	9.7704	16.5923	10.4184	**21.3109**
	D=75	6.6418	9.8955	8.8751	16.2338	10.1870	**20.7676**
	D=80	6.3710	9.5853	8.0166	16.0896	10.0540	**19.8456**
	D=85	6.1097	9.2949	7.2402	16.0498	10.4173	**19.1445**
	D=90	5.8582	9.0214	6.5767	16.2932	11.2993	**18.9571**

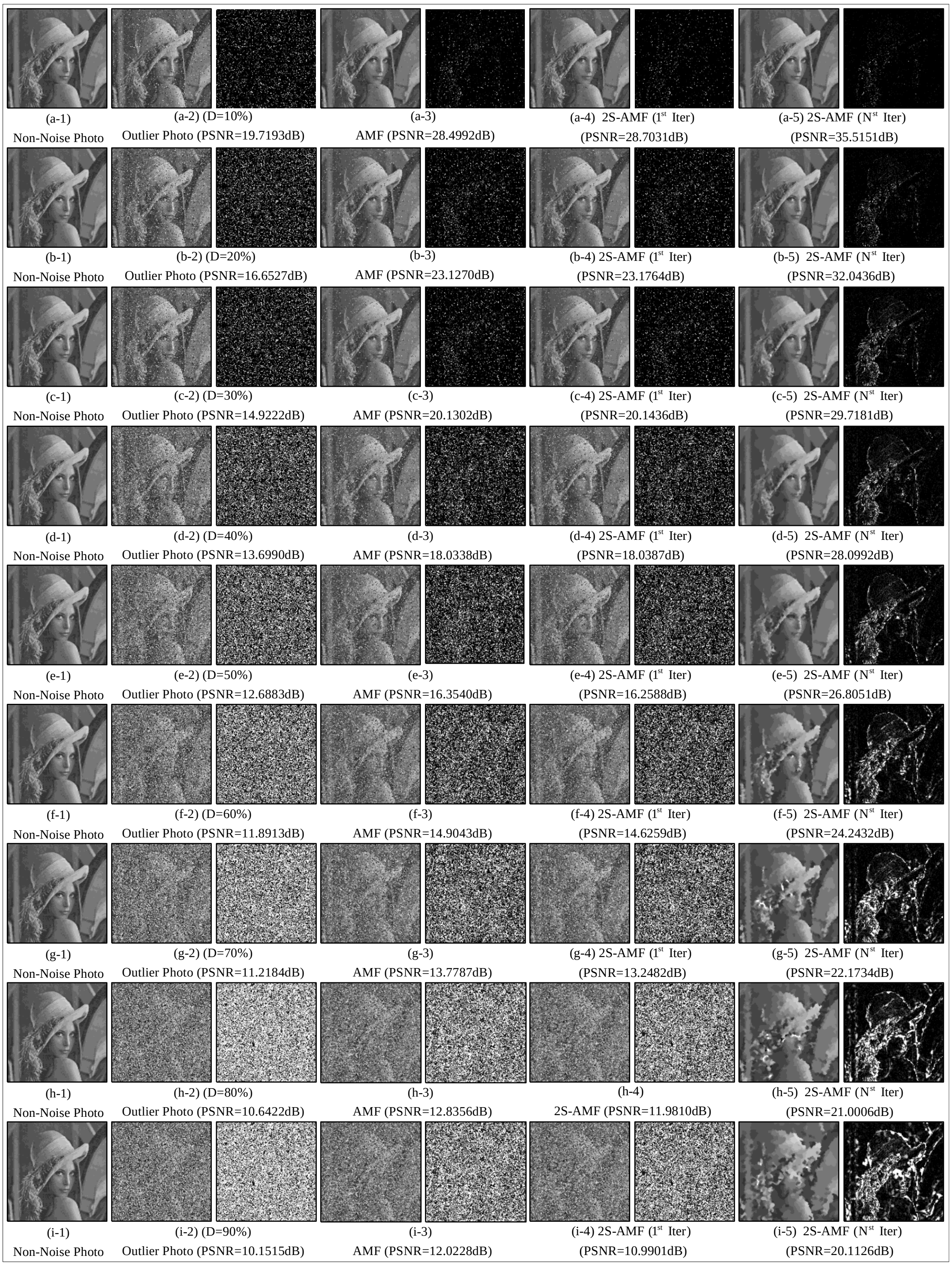

Figure 3. The experimental results of irregularity reduction algorithm built on 2-stage and AMF (Lena)

5. CONCLUSION

This paper attempts to proposes the alternative irregularity reduction algorithm built on a 2-stage identification and AMF for FMIO (fix magnitude impulsive outlier) at from 5% to 90% massiveness. The first contribution of this paper is the simulated determination of the optimized window dimension for 2-stage scheme, which are simulated from 3 standard digital depictions (Lena, Girl and Pepper) at from all massiveness (5% to 90%). The second contribution of this paper is the statistical characteristic examination (the expectation and the SD) of 2-stage identification between regular and irregular pixels at all massiveness.

From the previous the optimal window size of 2-stage scheme, the third contribution of this paper is the optimal 2-stage constant of outlier reduction built on 2-stage technique and AMF. Finally, the overall efficacy of the 2-stage outlier reduction algorithm built on 2-stage and AMF comparatively examined with other up-to-the-minute outlier reduction algorithms such as MF, SMF and AMF on FMIO. From these results, the outlier reduction built on 2-stage technique and AMF has remarkable efficacy than other up-to-the-minute outlier reductions such as SMF, GF and AMF on FMIO.

REFERENCES

[1] R. C. Gonzalez and R. E. Woods, *Digital Image Processing*, 2nd ed., Upper Saddle River, *NJ, USA*, Prentice-Hall, 2002.

[2] A. S. M. Shafi and M. M. Rahman, "Decomposition of color wavelet with higher order statistical texture and convolutional neural network features set based classification of colorectal polyps from video endoscopy," *International Journal of Electrical and Computer Engineering (IJECE)*, vol. 10, no. 3, pp. 2986-2996, 2020, doi: 10.11591/ijece.v10i3.pp2986-2996.

[3] S. Bagchi, K. G. Tay, A. Huong, and S. K. Debnath, "Image processing and machine learning techniques used in computer-aided detection system for mammogram screening-A review," *International Journal of Electrical and Computer Engineering (IJECE)*, vol. 10, no. 3, pp. 2336-2348, 2020, doi: 10.11591/ijece.v10i3.pp2336-2348.

[4] N. D. Abdullah, U. R. Hashim, S. Ahmad, and L. Salahuddin, "Analysis of texture features for wood defect classification," *Bulletin of Electrical Engineering and Informatics (BEEI)*, vol. 9, no. 1, pp. 121-128, 2020, doi: 10.11591/eei.v9i1.1553.

[5] A. J. Qasim, R. Din, and F. Q. A. Alyousuf, "Review on techniques and file formats of image compression," *Bulletin of Electrical Engineering and Informatics (BEEI)*, vol. 9, no. 2, pp. 602-610, 2020, doi: 10.11591/eei.v9i2.2085.

[6] S. P. Ramalingam, R. K. Nadesh, and N. C. S. Kumar, "Robust face recognition using enhanced local binary pattern," *Bulletin of Electrical Engineering and Informatics (BEEI)*, vol. 7, no. 1, pp. 96-101, 2018, doi: 10.11591/eei.v7i1.761.

[7] V. H. Patil, G. K. Kharate, and K. S. Mohan, "Super resolution imaging needs better registration for better quality results," *Bulletin of Electrical Engineering and Informatics (BEEI)*, vol. 1, no. 1, pp. 43-50, 2012, doi: 10.11591/eei.v1i1.225.

[8] C. Deng, J. Liu, W. Tian, S. Wang, H. Zhu, and S. Zhang, "Image super-resolution reconstruction based on L1/2 sparsity," *Bulletin of Electrical Engineering and Informatics (BEEI)*, vol. 3, no. 3, pp. 2014, doi: 10.11591/eei.v3i3.284.

[9] D. Kesrarat, K. Thakulsukanant, and V. Patanavijit, "A novel elementary spatial expanding scheme form on SISR method with modifying Geman&McClure function," *TELKOMNIKA (Telecommunication Computing Electronics and Control)*, vol. 17, no. 5, pp. 2554-2560, 2019, doi: 10.12928/telkomnika.v17i5.12799.

[10] I. Pitas, A. N. Venetsanopoulos, "Median filters," in *Nonlinear Digital Filters*, Boston, MA, Springer, 1990.

[11] J. Astola, P. Haavisto, and Y. Neuvo, "Vector median filters," *Proceedings of the IEEE*, vol. 78, no. 4, pp. 678-689, 1990, doi: 10.1109/5.54807.

[12] H. Hwang and R. A. Haddad, "Adaptive median filters new algorithms and results," *IEEE Transactions on Image Processing*, vol. 4, no. 4, pp. 499-502, 1995, doi: 10.1109/83.370679.

[13] O. P. Verma and N. Sharma, "Intensity preserving cast removal in color images using particle swarm optimization," *International Journal of Electrical and Computer Engineering (IJECE)*, vol. 7, no. 5, pp. 2581-2595, 2017, doi: 10.11591/ijece.v7i5.pp2581-2595.

[14] M. Hamiane and F. Saeed, "SVM classification of MRI brain images for computer-assisted diagnosis," *International Journal of Electrical and Computer Engineering (IJECE)*, vol. 7, no. 5, pp. 2555-2564, 2017, doi: 10.11591/ijece.v7i5.pp2555-2564.

[15] A. Khmag, S. Ghoul, S. A. R. Al-Haddad, and N. Kamarudin, "Noise level estimation for digital images using local statistics and its applications to noise removal," *TELKOMNIKA (Telecommunication Computing Electronics and Control)*, vol. 16, no. 2, pp. 915-924, 2018, doi: 10.12928/telkomnika.v16i2.9060.

[16] K. A. Sai, and K. Ravi, "An efficient filtering technique for denoising colour images," *International Journal of Electrical and Computer Engineering (IJECE)*, vol. 8, no. 5, pp. 3604-3608, 2018, doi: 10.11591/ijece.v8i5.pp3604-3608.

[17] Z. M. Ramadan, "Effect of kernel size on Wiener and Gaussian image filtering," *TELKOMNIKA (Telecommunication Computing Electronics and Control)*, vol. 17, no. 3, pp. 1455-1460, 2019, doi: 10.12928/telkomnika.v17i3.11192.

[18] J. Na'am, J. Harlan, R. Syelly, and A. Ramadhanu, "Filter technique of medical image on multiple morphological gradient (MMG) method," *TELKOMNIKA (Telecommunication Computing Electronics and Control)*, vol. 17, no. 3, pp. 1317-1323, 2019, doi: 10.12928/telkomnika.v17i3.9722.

[19] B. Charmouti *et al*., "An overview of the fundamental approaches that yield several image denoising techniques," *TELKOMNIKA (Telecommunication Computing Electronics and Control)*, vol. 17, no. 6, pp. 2959-2967, 2019, doi: 10.12928/telkomnika.v17i6.11301.

[20] L. Abderrahim, M. Salama, and D. Abdelbaki, "Novel design of a fractional wavelet and its application to image denoising," *Bulletin of Electrical Engineering and Informatics (BEEI)*, vol. 9, no. 1, pp. 129-140, 2020, doi: 10.11591/eei.v9i1.1548.

[21] Y. Y. Al-Aboosi, R. S. Issa, and A. K. Jassim, "Image denosing in underwater acoustic noise using discrete wavelet transform with different noise level estimation," *TELKOMNIKA (Telecommunication Computing Electronics and Control)*, vol. 18, no. 3, pp. 1439-1446, 2020, doi: 10.12928/telkomnika.v18i3.14381.

[22] S. Rajkumar and G. Malathi, "An efficient image denoising approach for the recovery of impulse noise," *Bulletin of Electrical Engineering and Informatics (BEEI)*, vol. 6, no. 3, pp. 281-286, 2017, doi: 10.11591/eei.v6i3.680.

[23] V. Patanavijit, "Denoising performance analysis of adaptive decision based inverse distance weighted interpolation (DBIDWI) algorithm for salt and pepper noise," *Indonesian Journal of Electrical Engineering and Computer Science (IJEECS)*, vol. 15, no. 2, pp. 804-813, 2019, doi: 10.11591/ijeecs.v15.i2.pp804-813.

[24] V. Kishorebabu, G. Packyanathan, H. Kamatham, and V. Shankar, "An adaptive decision based interpolation scheme for the removal of high density salt and pepper noise in images," *EURASIP Journal on Image and Video Processing*, vol. 2017, 2017, doi: 10.1186/s13640-017-0215-0.

[25] V. Patanavijit and K. Thakulsukanant, "The statistical analysis of random-valued impulse noise detection techniques based on the local image characteristic: ROAD, ROLD and RORD," *Indonesian Journal of Electrical Engineering and Computer Science (IJEECS)*, vol. 15, no. 2, pp. 794-803, 2019, doi: 10.11591/ijeecs.v15.i2.pp794-803.

[26] C. Lin, Y. Li, S. Feng and M. Huang., "A two-stage algorithm for the detection and removal of random-valued impulse noise based on local similarity," *IEEE Access*, vol. 8, pp. 222001-222012, 2020, doi: 10.1109/ACCESS.2020.3040760.

BIOGRAPHIES OF AUTHORS

Vorapoj Patanavijit received the B.Eng., M.Eng. and Ph.D. degrees from the Department of Electrical Engineering at the Chulalongkorn University, Bangkok, Thailand, in 1994, 1997 and 2007 respectively. He has served as a full-time lecturer at Department of Electrical and Electronic Engineering, Faculty of Engineering, Assumption University since 1998 where he is currently an Associate Professor. He has authored and co-authored over 180 national/international peer-reviewed publications in Digital Signal Processing (DSP) and Digital Image Processing (DIP). He received the best paper awards from many conferences such as ISCIT2006 (2006), NCIT2008 (2008), EECON-33 (2010), EECON-34 (2011), EECON-35 (2012), and EECON-43 (2020). Moreover, he is invited to be the guest speaker at IWAIT2014 and contributed the invited paper at iEECON 2014. As a technical reviewer of international journals since 2006, he has been assigned to review over 100 journal papers (indexed by SCI and Scopus). As a technical reviewer of over 40 international/national conferences since 2006, he has been assigned to review over 175 proceeding papers. He has participated in more than 8 projects and research programmed funded by public and private organizations. He works in the field of signal processing and multidimensional signal processing, specializing, in particular, on image/video reconstruction, SRR (super-resolution reconstruction), compressive sensing, enhancement, fusion, digital filtering, denoising, inverse problems, motion estimation, optical flow estimation and registration. He can be contacted at email: patanavijit@yahoo.com.

Darun Kesrarat received the B.S., M.S., and Ph.D. from the Department of Information Technology at Assumption University, Bangkok, Thailand. He is currently an Assistance Professor. His research areas include signal processing on image/video reconstruction, SRR (super-resolution reconstruction), motion estimation, and optical flow estimation. He can be contacted at email: darunksr@gmail.com.

Kornkamol Thakulsukanant received the B.Eng. (Electrical Engineering) from Assumption University, Thailand in 1994, MSc. (Telecommunications and Computer Network Engineering) from London South Bank University, United Kingdom in 1997 and Ph.D. (in Electronic and Electrical Engineering) from Bristol University, United Kingdom in 2009 respectively. She works in the field of digital signal processing (DSP) and digital image processing (DIP), specializing, in particular, on digital image reconstruction/enhancement. She can be contacted at email: kthakulsukanant@yahoo.com.